A Novel Approach to Reduce Dynamic Interactions in Space Robots

ERIC MARTIN
Space Technologies,
Canadian Space Agency,
St-Hubert, Quebec J3Y 8Y9
Eric.Martin@space.gc.ca

EVANGELOS PAPADOPOULOS
Department of Mechanical Engineering,
National Technical University of Athens,
15773 Athens, Greece
egpapado@central.ntua.gr

JORGE ANGELES
Department of Mechanical Engineering
McGill University,
Montreal, Quebec H3A 2K6
angeles@cim.mcgill.ca

ABSTRACT

Space manipulators mounted on an on-off thruster-controlled base are envisioned to assist in the assembly and maintenance of space structures. When handling large payloads, manipulator joint and link flexibility become important, for they can result in payload-attitude controller, fuel-replenishing dynamic interactions. In this paper, the describing-function concept is adapted to be used in conjunction with the root-locus concept, thus providing a different picture of the problem and helping in the control system design. This novel adaptation of the describing-function method has shown to give better physical insight in the understanding of the dynamic interaction problem and the design of control schemes to eliminate it.

KEY WORDS: *Space Robots, Dynamic Interaction, Describing-Function, Thrusters*

INTRODUCTION

Robotic devices in orbit will play an important role in space exploration and exploitation. Their mobility can be enhanced by mounting them on free-flying bases, controlled by on-off thrusters. Such robots introduce a host of dynamic and control problems not found in terrestrial applications. When handling large payloads, manipulator joint or structural flexibility becomes important and can result in payload-attitude controller, fuel-replenishing dynamic interactions. Such interactions may lead to control system instabilities, or manifest themselves as limit cycles [1].

The CANADARM-Space Shuttle system is the only operational space robotic system to date. Its Reaction Control System (RCS), which makes use of on-off thrusters, is designed assuming rigid-body motion, and using single-axis, thruster switching logic based on phase-plane techniques. This approach is common in the design of thruster-based control systems. However, the flexible modes of this space robotic system have rather low frequencies, which continuously change with manipulator configuration and payload, and can be excited by the RCS activity. Currently, the method for resolving these problems consists of performing extensive simulations. If dynamic interactions occur, corrective actions are taken, which would include adjusting the RCS parameter values, or simply changing the operational procedures [2]. The describing-function method has also been used to study this highly nonlinear problem due to the use of on-off thrusters. The method was used to analyze the problem of payload deployment by means of a tilt table [3]. Stability maps were obtained and compared to simulation results to validate the describing-function analysis. On-off pulse modulator attitude control system were designed in [4] using the describing-function analysis for a spacecraft having large flexible solar arrays. They used the relative stability margin, with respect to the limit-cycle condition of a structural mode, as a measure of the robustness of the nonlinear control system. Using the same idea, it was shown in [5] that the describing-function analysis can be utilized for practical control design problems such as flexible spacecraft equipped with pulse-modulated reaction jets.

Although the describing-function technique is a good tool to analyze the stability of this kind of systems, it gives very little physical insight in the nature of the problem and the design of new control schemes to eliminate it. In this paper, the describing-function concept is adapted to be used in conjunction with the root-locus method well known in linear control theory. This novel adaptation of the describing-function concept has been used in [6] to design three new control schemes that can eliminate the problem of dynamic interactions. Its interest comes with the physical insight it can provide on the nature of the problem, thus allowing the design of more efficient control schemes.

SYSTEM DESCRIPTION

Dynamics Modeling

The dynamics model of the N-flexible-joint space manipulator depicted in Fig. 1(a) was developed using a Lagrangian formulation under the assumption that all link and joint flexibilities are lumped at the joints [6]. This is reasonable, since joint flexibility is more signif-

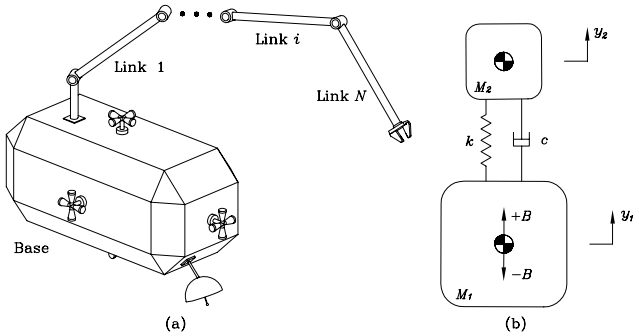

Figure 1: (a) A space manipulator system; (b) A simplified two-mass system.

icant than link flexibility in this kind of system. Each flexible joint is modeled as a torsional spring in parallel to a torsional dashpot. Using linearization techniques, the natural frequency and damping ratio expressions for this system were obtained as functions of the configuration of the manipulator, [6].

However, the dynamics of this space manipulator is rather complicated; it is preferable to employ a simplified model to analyze the problem stated in the introduction. We can replace the manipulator of Fig. 1(a) with an equivalent two-mass-spring-dashpot system, as shown in Fig. 1(b). By a proper selection of the spring stiffness k and the damping coefficient c, the resonant frequency of the simplified system can be matched to the first one of the original system. Therefore, a similar relative motion of the payload with respect to the base can be obtained.

The equations of motion for the system shown in Fig. 1(b) can be readily derived as

$$M_1\ddot{y}_1 + c(\dot{y}_1 - \dot{y}_2) + k(y_1 - y_2) = f(t) \quad (1a)$$

$$M_2\ddot{y}_2 - c(\dot{y}_1 - \dot{y}_2) - k(y_1 - y_2) = 0\,, \quad (1b)$$

where M_1 is the mass of the base, M_2 the mass of the payload, y_1 the position of the base, y_2 the position of the payload, k the spring stiffness, c the damping coefficient, $f(t) = Bu$, with B the magnitude of the force developed by the thrusters, and u is the command of the thrusters, either $+1$, 0 or -1.

The overall motion of the system can be decomposed into a rigid-body motion of the system center of mass (CM), and a flexible-body motion around the center of mass, defining the resonant frequency ω_n, the damping ratio ζ, and the reduced mass μ as

$$\omega_n = \sqrt{\frac{k}{\mu}}\,, \qquad \zeta = \frac{c}{2\sqrt{\mu k}}\,, \qquad \mu = \frac{M_1 M_2}{M_1 + M_2}\,. \quad (2)$$

From Eq.(2), we obtain the system stiffness k and damping coefficient c, as

$$k = \mu\omega_n^2, \qquad c = 2\mu\zeta\omega_n\,. \quad (3)$$

Therefore, using Eq.(3), k and c can be chosen to match a specific resonant frequency ω_n and a damping ratio ζ for given masses M_1 and M_2.

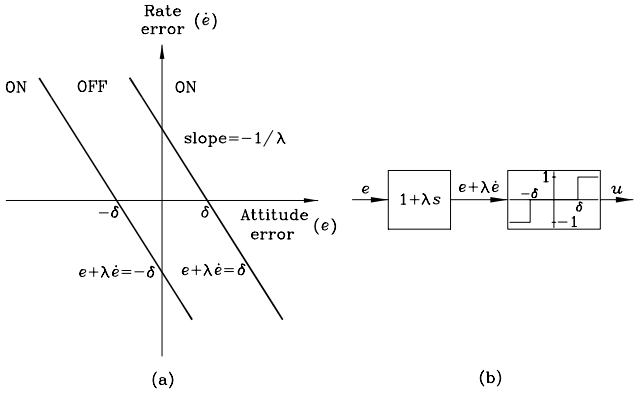

Figure 2: (a) Switching logic in the error phase plane; (b) Controller block.

The transfer function $G_p(s)$ mapping the input u into the base position y_1, namely

$$Y_1(s) = G_p(s)U(s) \quad (4)$$

can be derived as

$$G_p(s) = \gamma\frac{(1+\beta)s^2 + 2\zeta\omega_n s + \omega_n^2}{s^2(s^2 + 2\zeta\omega_n s + \omega_n^2)} \quad (5)$$

where the mass ratio β and the acceleration of the CM γ are given by

$$\beta = M_2/M_1, \qquad \gamma = \gamma_0/(1+\beta) \quad (6)$$

γ_0 being the nominal acceleration that can be provided by the thrusters when $\beta = 0$.

Controller Structure

The technology currently available does not allow the use of proportional thruster valves in space, and thus, classical PD and PID control laws cannot be used; spacecraft attitude and position are controlled by on-off thruster valves, that introduce nonlinearities.

The usual scheme to control a spacecraft with on-off thrusters employs the error phase plane, defined as having the spacecraft attitude error e and error rate $\dot{e}$ as coordinates. The on-and-off switching is determined by switching lines in the phase plane and can become complex, as for example, the phase plane controller of the Space Shuttle [2]. To simplify the switching logic, two switching lines with equations $e + \lambda\dot{e} = \pm\delta$ have been used, as shown in Fig. 2(a). The deadband limits $[-\delta, \delta]$ are determined by attitude limit requirements, while the slope of the switching lines, by the desired rate of convergence towards the equilibrium and by the rate limits. This switching logic can be represented as a relay with a deadband, where the input is $e + \lambda\dot{e}$, the left-hand side of the switching-line equations, see Fig. 2(b).

To compute the input to the controller, the position and the velocity of the base are required and can be obtained from sensors. However, it can happen that only

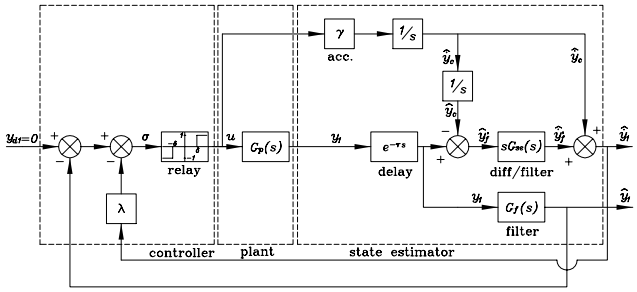

Figure 3: Model with a classical rate estimator.

the attitude is available and then, the angular velocity must be estimated. As shown in [7], the use of sensors to obtain the rate of the base may deteriorate the performance of the system due to the high-frequency filtering requirements. Here, we consider that only the attitude is available from sensors, and, hence, to obtain the velocity, estimators are used.

In this paper, a controller-plant-estimator configuration similar to the one used on the Space Shuttle is employed [2]. A differentiator combined with a second-order filter is used to obtain a velocity estimate, as shown in Fig. 3. The differentiation of a noisy signal is not recommended because it amplifies noise. However, in this case, it is possible to use a scheme where only the flexible part of the motion needs to be differentiated. This means that, at the limit, for a rigid system, no differentiation is necessary. This state estimator can give very good results when flexibility is low. The differentiator-filter is given by $sG_{se}(s)$ where

$$G_{se}(s) = \frac{\omega_{se}^2}{s^2 + 2\zeta_{se}\omega_{se}s + \omega_{se}^2} \tag{7}$$

The attitude feedback is also low-pass-filtered using a second-order filter represented by $G_f(s)$

$$G_f(s) = \frac{\omega_f^2}{s^2 + 2\zeta_f\omega_f s + \omega_f^2} \tag{8}$$

For this filter, we use $\omega_f = 0.47$ rad/s and $\zeta_f = 0.707$, while, for the differentiator-filter, we use values that correspond to the ones used on the Space Shuttle [2], namely, $\omega_{se} = 0.2513$ rad/s and $\zeta_{se} = 0.707$.

FREQUENCY-DOMAIN ANALYSIS

Describing-Function Method

Since the attitude controller assumes use of on-off thrusters, which are nonlinear devices, the system cannot be adequately analyzed through the application of linear analysis methods. This problem is solved using the describing-function method, which can predict the existence of limit cycles in nonlinear systems [8, 9].

In order to use this method, the system under study must be partitioned into a linear and a nonlinear part.

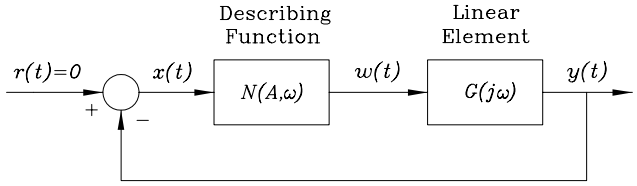

Figure 4: A nonlinear system analyzed with describing functions.

Then, it is transformed into the configuration shown in Fig. 4. $G(j\omega)$ is the frequency response of all the linear elements in the system and $N(A,\omega)$ is the describing function of the nonlinearity, which is tabulated in many books, e.g., in [9].

The characteristic equation of the system depicted in Fig. 4 can be written as

$$G(j\omega) = -\frac{1}{N(A,\omega)} \tag{9}$$

The reader is refered to [8] and [9] for a detailed description of the method. In summary, if a given set of A and ω is a solution of Eq.(9), then the system exhibits a limit cycle of amplitude A and frequency ω. If the above equation has no solution, then the nonlinear system has no limit cycle. A convenient way to solve Eq.(9) consists of plotting both sides of the equation in the complex plane by varying A and ω, and observing whether the two curves intersect or not. An intersection point will provide the corresponding values of A and ω. Furthermore, one has to investigate the stability properties of the limit cycle and the general behavior of the system [9]. For example, Fig. 5 depicts three typical describing-function plots encountered in this work, where the describing function N of the relay is a function of the gain A only. Figure 5(a) is typical of an unstable system where the motion diverges, none of the intersection points representing a stable limit cycle. Figure 5(b) depicts a system that sustains a limit cycle of amplitude A and frequency ω due to the dynamic interactions. Finally, Fig. 5(c) shows a stable case where the motion reaches a small unavoidable limit cycle. Figures 5(a) and (b) both correspond in high thruster activity. This behavior is not desirable in space missions, and should therefore be classified as unstable.

Root-Locus Method

Alternatively, in this paper, the describing-function concept was adapted for the analysis of space robotic systems controlled with on-off thrusters via the root-locus method. The characteristic equation of the system, eq.(9), can be written as

$$q(s) + N(A,\omega)p(s) = 0 \tag{10}$$

where $p(s)$ and $q(s)$ are respectively the numerator and denominator of the transfer function $G(s)$ of all

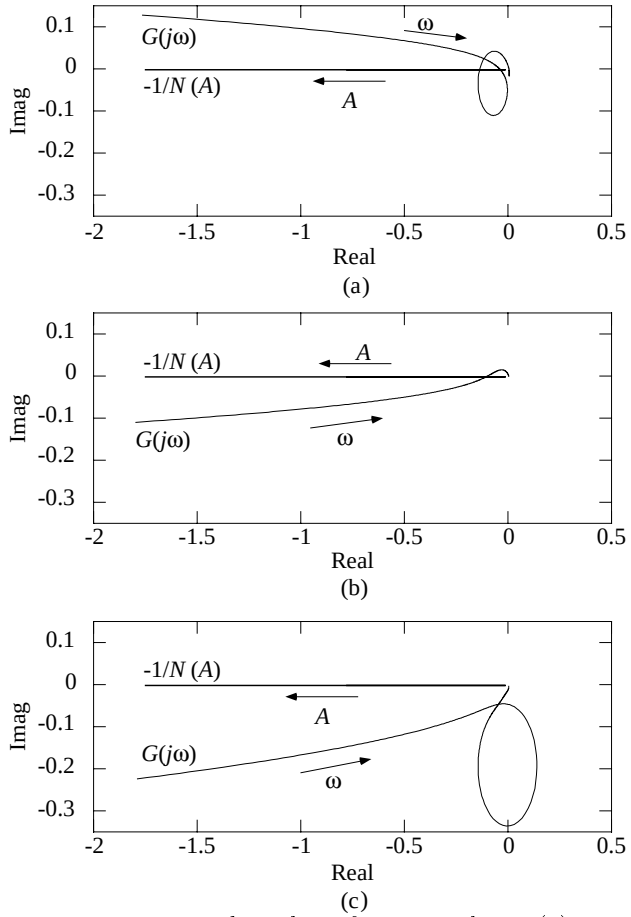

Figure 5: Typical describing-function plots: (a) Unstable system; (b) Limit-cycling system; and (c) Stable system.

the linear elements of the system. Equation (10) has the standard form used for the root-locus concept by replacing the varying parameter K by the describing function of the nonlinear element of our system $N(A, \omega)$. The varying parameters thus become the amplitude A and the frequency ω of the assumed limit cycle. For the case where the describing function is only a function of the amplitude A, which is the case for a relay nonlinearity, and thus for the case under study in this paper, the locus of the closed-loop poles in the complex plane is obtained by varying solely this parameter. We thus have

$$q(s) + N(A)p(s) = 0 \tag{11}$$

Moreover, let us assume that the i-th root of Eq.(11) is

$$s_i = \sigma_i + j\omega_i \tag{12}$$

when A has the value A_i. Thus, from Eq.(11), we have

$$q(\sigma_i + j\omega_i) + N(A_i)p(\sigma_i + j\omega_i) = 0 \tag{13}$$

We can further assume that for the given A_i, the root s_i is on the $j\omega$-axis. Hence,

$$\sigma_i = 0 \tag{14}$$

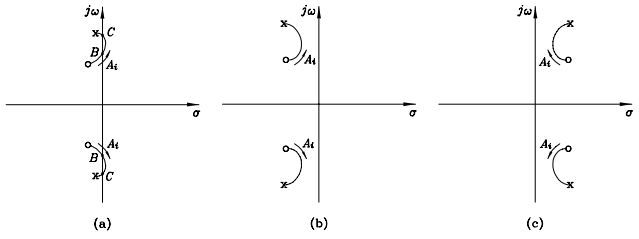

Figure 6: Stability prediction using the root-locus method. (a) Unstable limit-cycling system, (b) Stable system, (c) Unstable system with diverging motion.

and Eq.(13) becomes

$$q(j\omega_i) + N(A_i)p(j\omega_i) = 0 \tag{15}$$

which can be written as

$$\frac{p(j\omega_i)}{q(j\omega_i)} = G(j\omega_i) = -\frac{1}{N(A_i)} \tag{16}$$

Equation (16) thus has the same form as Eq.(9) and hence corresponds to the intersection of the two loci $G(j\omega)$ and $-1/N(A)$. Therefore, when a branch of the root-locus plot crosses the $j\omega$-axis at a certain ω_i, for a given value A_i, then the system exhibits a limit cycle of amplitude A_i and frequency ω_i. The stability of this limit cycle can be assessed by considering points of the loci near the intersection point. For the root-locus method applied to nonlinear systems, the following Limit Cycle Criterion was developed:

Limit Cycle Criterion: *Each intersection point of a locus of the root-locus plot with the $j\omega$-axis corresponds to a limit cycle. Assuming a stable $G(s)$, if points near the intersection and along the increasing-A side of the locus are in the left-half plane, then the corresponding limit cycle is stable. Otherwise, the limit cycle is unstable.*

For example, points B of Fig. 6(a) correspond to an unstable limit cycle, and points C correspond to a stable one.

On the other hand, if none of the loci intersects the $j\omega$-axis, the system is stable if all the loci are in the left-half plane, and it is unstable with a diverging motion if one or more of the loci is completely in the right-half plane, which means that there exists at least one pole of the closed-loop system with its real part being positive, for any value of A. For example, assuming that $G(j\omega)$ is stable, Fig. 6(b) depicts a stable system while Fig. 6(c) an unstable one.

EXAMPLE: THE TWO-MASS SYSTEM

The interaction problem identified in the introduction is analyzed here using the describing-function and the root-locus methods, for the two-mass system of Fig. 1(b). For the classical rate estimator of Fig. 3,

the transfer function of the linear elements $G_{\text{rate}}(s)$ (Fig. 4) is derived in [6] and is given by

$$G_{\text{rate}}(s) = e^{-\tau s} G_p(s)\big(G_f(s) + \lambda s G_{se}(s)\big) + \frac{\lambda\gamma}{s}\big(1 - G_{se}(s)\big) \tag{17}$$

where $G_p(s)$, $G_{se}(s)$ and $G_f(s)$ are defined in Eqs.(5), (7), and (8), respectively. The plant transfer function is represented by $G_p(s)$, while $G_f(s)$ and $G_{se}(s)$ are the transfer functions of second-order filters. Finally, for the root-locus analysis, the delay τ is represented as a third-order Padé approximation, namely,

$$e^{-\tau s} = \frac{2 - \tau s + \tau^2 s^2/2 - \tau^3 s^3/6}{2 + \tau s + \tau^2 s^2/2 + \tau^3 s^3/6} \tag{18}$$

We consider a configuration of a three-link version of the manipulator of Fig. 1(a) given by

$$\theta_1 = 120^\circ, \quad \theta_3 = 90^\circ, \quad \theta_5 = 105^\circ$$

and two different payloads

$$\text{i) } \beta = 0.05 \qquad \text{ii) } \beta = 0.3$$

Considering, link lengths and mass properties of this system based on the CANADARM/Space Shuttle system, the first natural mode and damping ratio of the system for these β values are obtained in [6] as

$$\begin{aligned} &\text{i) } \omega_1 = 2\pi(0.096) \text{ rad/s}, && \zeta_1 = 0.015 \\ &\text{ii) } \omega_2 = 2\pi(0.053) \text{ rad/s}, && \zeta_2 = 0.008 \end{aligned}$$

Therefore, we consider the two-mass system with two sets of parameters:

$$\begin{aligned} &\text{i) } \beta = 0.05, \quad \omega_n = 2\pi(0.096) \text{ rad/s}, \quad \zeta = 0.015 \\ &\text{ii) } \beta = 0.3, \quad \omega_n = 2\pi(0.053) \text{ rad/s}, \quad \zeta = 0.008 \end{aligned}$$

Moreover, for this study, we choose

$$\lambda = 5 \text{ s}, \quad \delta = 0.01 \text{ m}, \quad \gamma_0 = 0.01 \text{ m/s}^2, \quad \tau = 0.1 \text{ s}$$

The plots obtained using the describing-function technique outlined above are displayed in Fig. 7(a) for the $\beta = 0.05$ case and in Fig. 8(a) for the $\beta = 0.3$ case. Similarly, the root-locus plots obtained using the root-locus analysis with the amplitude A of the predicted limit cycle as the varying parameter, are displayed in Figs. 7(b) and (c), and in Figs. 8(b) and (c), respectively, for the $\beta = 0.05$ case and the $\beta = 0.3$ case. From Fig. 7(a), it is clear that the system is stable since none of the points of the $-1/N(A)$ locus is encircled by the $G(j\omega)$ locus. The same conclusion is obviously obtained by looking at Figs. 7(b) and (c), since none of the closed-loop poles lies in the right-half plane. Obviously, Figs. 7(a)–(c) correspond to two different pictures of the same problem.

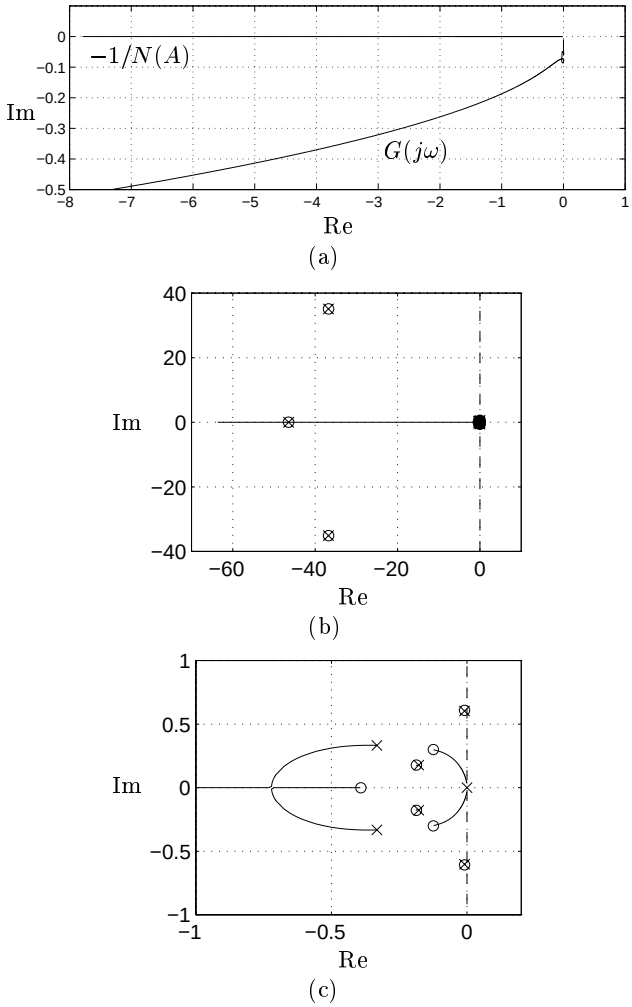

Figure 7: Theoretical analysis with the classical rate estimator for the $\beta = 0.05$ case: (a) describing-function plot; (b) root-locus plot; and (c) root-locus plot (zoom).

On the other hand, by looking at Fig. 8(a), we see that the system is unstable and will be limit-cycling with a high amplitude motion, since the $-1/N(A)$ and $G(j\omega)$ loci intersect, the intersection point corresponding to a stable limit cycle.

The same conclusion is drawn when looking at Figs. 8(b) and (c), where two loci go into the right-half plane, thus corresponding to positive closed-loop poles, and hence, to an unstable system.

It is very interesting to compare Figs. 7(b) and (c) with Figs. 8(b) and (c). We know that the effect of increasing the payload, or equivalently, of β, is to lower the natural frequency of the system, and thus, the poles and zeros corresponding to this frequency move towards the real axis in the root-locus plot, namely, those in the upper right part of Figs. 7(c) and 8(c). From Fig. 7(c), it is apparent that these poles and zeros do not interfere with those of the filters $G_f(s)$ and $G_{se}(s)$. However, as β increases, the locus completely changes and the dynamics of the plant interferes with

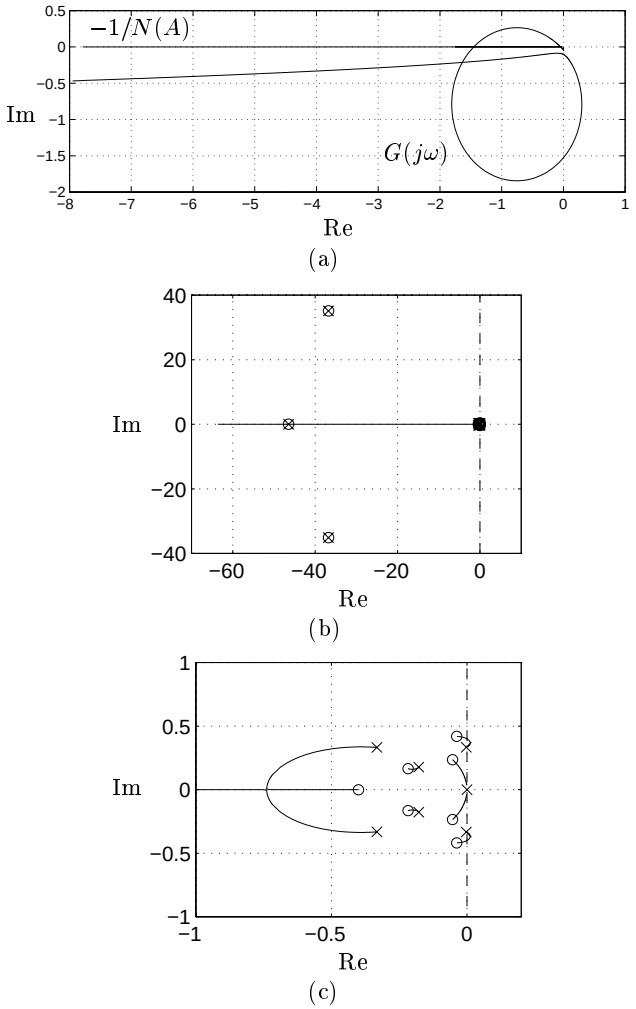

Figure 8: Theoretical analysis with the classical rate estimator for the $\beta = 0.3$ case: (a) describing-function plot; (b) root-locus plot; and (c) root-locus plot (zoom).

the dynamics of the filters, as shown in Fig. 8(c), the result being that two loci cross the imaginary axis into the right-half plane. From this analysis, it becomes clear that any controller designed to avoid such interference would improve the system stability. This analysis using the root-locus plots is very important in understanding the problem at hand and in finding solutions to eliminate it. This new design tool was used in [6] to develop three new estimation schemes that solve the problem of dynamic interactions.

CONCLUSION

This work examined possible dynamic interactions between the attitude controller of a spacecraft and the flexible modes of a space manipulator mounted on it. Using a simplified model of the plant, namely, a two-mass system, the describing-function method was used to investigate the stability of the system. A novel adaptation of this analysis method for nonlinear systems was presented. This adaptation uses the describing functions in conjunction with the root-locus method. It has the advantage of providing a different picture of the problem resulting in better physical insight in the understanding of the dynamic interaction problem. It also provides a valuable tool for the design of new control schemes to eliminate that problem.

ACKNOWLEDGEMENTS

The support of this work by Quebec's Fonds pour la Formation de Chercheurs et l'Aide à la Recherche (FCAR) and by Canada's Natural Sciences and Engineering Council (NSERC) is gratefully acknowledged.

REFERENCES

[1] Millar, R. A., and Vigneron, F. R., "Attitude Stability of a Pseudorate Jet-Controlled Flexible Spacecraft," *J. Guid., Cont., and Dyn.*, Vol. 2, No. 2, 1979, pp. 111–118.

[2] Sackett, L. L., and Kirchwey, C. B., "Dynamic Interaction of the Shuttle On-Orbit Flight Control System with Deployed Flexible Payload," *Proc. AIAA Guid., and Cont. Conf.*, San Diego, CA, 1982, pp. 232–245.

[3] Penchuk, A. N., Hattis, P. D., and Kubiak, E. T., "A Frequency Domain Stability Analysis of a Phase Plane Control System," *J. Guid., Cont., and Dyn.*, Vol. 8, No. 1, 1985, pp. 50–55.

[4] Wie, B., and Plescia, C. T., "Attitude Stabilization of Flexible Spacecraft During Stationkeeping Maneuvers," *J. Guid., Cont., and Dyn.*, Vol. 7, No. 4, 1984, pp. 430–436.

[5] Anthony, T. C., Wie, B., and Carroll, S., "Pulse-Modulated Control Synthesis for a Flexible Spacecraft," *J. Guid., Cont., and Dyn.*, Vol. 13, No. 6, 1990, pp. 1014–1022.

[6] Martin, E., "Dynamic Interaction of a Space Manipulator with its Base Attitude Controller," Ph.D. Thesis, Dept. of Mech. Eng., McGill University, Montreal, Canada, 1999.

[7] Martin, E., Papadopoulos, E., and Angeles, J., "On the Interaction of Flexible Modes and On-off Thrusters in Space Robotic Systems," *Proc. 1995 Int. Conf. Intelligent Robots and Systems, IROS'95*, Pittsburgh, PA, 1995, pp. 65–70.

[8] J.-J.E. Slotine and W. Li, 1991, *Applied Nonlinear Control*, Prentice Hall, N.J.

[9] D.P. Atherton, 1975, *Nonlinear Control Engineering*, Van Nostrand, New York.